Computing resonant modes of circular cylindrical resonators by vertical mode expansions

Hualiang Shi
School of Science, Hangzhou Dianzi University, Hangzhou, Zhejiang, China

Ya Yan Lu*
Department of Mathematics, City University of Hong Kong, Hong Kong, China

(Received 20 May 2019; published 8 July 2019)

Open subwavelength cylindrical resonators of finite height are widely used in various photonics applications. Circular cylindrical resonators are particularly important in nanophotonics, since they are relatively easy to fabricate and can be designed to exhibit different resonance effects. In this paper, an efficient and robust numerical method is developed for computing resonant modes of circular cylinders which may have a few layers and may be embedded in a layered background. The resonant modes are complex-frequency outgoing solutions of the Maxwell's equations with no sources or incident waves. The method uses field expansions in one-dimensional (1D) "vertical" modes to reduce the original three-dimensional eigenvalue problem to 1D problems and uses Chebyshev pseudospectral method to compute the 1D modes and set up the discretized eigenvalue problem. In addition, a new iterative scheme is developed so that the 1D nonlinear eigenvalue problems can be reliably solved. For metallic cylinders, the resonant modes are calculated based on analytic models for the dielectric functions of metals. The method is validated by comparisons with existing numerical results, and it is also used to explore subwavelength dielectric cylinders with high-Q resonances and analyze gold nanocylinders.

DOI: 10.1103/PhysRevE.100.013303

I. INTRODUCTION

Metallic or dielectric circular cylinders of finite height are widely used as optical resonators in photonics applications [1]. Depending on their material, size, and aspect ratio, circular cylinders are used in integrated photonics as microdisk resonators [2], in plasmonics as metallic nanoparticles, and in metasurfaces as building blocks [3–6]. Due to their simple geometry, circular cylinders are relatively easy to fabricate, and they are capable of creating strong local fields that are useful for lasing, sensing, Raman scattering, nonlinear optics, and quantum optics [1]. To design resonators of proper material, size, and aspect ratio and to analyze their applications, it is essential to calculate the resonant modes accurately. A resonant mode (also called resonant state or quasinormal mode) is a complex-frequency solution of the source-free Maxwell's equations satisfying an outgoing radiation condition. Some interesting resonant modes may exist at special geometric parameter values only. Recently, it was found that subwavelength dielectric cylinders of particular aspect ratio can have high-Q resonant modes [7] and these modes can be used to enhance second harmonic generation [8]. To find desired resonant modes for various applications, a robust, accurate, and efficient numerical method is needed. For metallic cylinders, the dielectric function depends strongly on the frequency. Since the resonant frequencies are complex, it is necessary to extend the dielectric function to the complex frequency plane using proper analytic models.

For dielectric cylindrical resonators, numerical methods that give the correct Q factors have appeared since 1980s [9,10]. Currently, the most widely used method is the finite-element method (FEM) with perfectly matched layers (PMLs) [11–13]. FEM is very versatile and its adaptive version is well suited to analyze structures with complex geometries [14]. PML is a widely used technique for truncating unbound domains in numerical simulations of waves [15]. For dielectric structures where the material dispersion can be ignored, FEM gives a linear matrix eigenvalue problem that can be solved using standard numerical linear algebra techniques. For dispersive media, the eigenvalue problem is nonlinear, but it can be linearized by using auxiliary functions if an analytic model for the dielectric function is available [16,17]. Typically, FEM gives rise to large matrices and it is not as efficient as desired. More efficient methods can be developed by taking advantage of the special features of the structure. The boundary integral equation (BIE) method is suitable for structures with a piecewise constant dielectric function [10,18], but it is complicated to implement when the cylinder and/or its surrounding have multiple layers. The Fourier modal method (FMM), also called rigorous coupled wave analysis, is widely used in diffraction analysis of layered periodic structures [19–21], and it has been extended to computing resonant modes of nonperiodic structures [22]. When applied to circular cylinders, the standard FMM [22,23] uses vectorial modes that are functions of the two horizontal variables (perpendicular to the cylinder axis) and avoids a discretization in the vertical variable z (along the cylinder axis). To take advantage of the rotational symmetry of circular cylinders, two special FMMs have been developed. The method of Armaroli *et al.* [24] and

*Corresponding author: mayylu@cityu.edu.hk

Bigourdan *et al.* [25] uses one-dimensional (1D) modes that depend on z and analytic solutions in the horizontal radial variable r and azimuthal angle θ. The method of Li *et al.* [26] uses 1D modes that depend on r and analytic solutions in z and θ. All versions of BIE and FMM give rise to fully nonlinear eigenvalue problems.

In this paper, we develop a simple 1D mode expansion method for analyzing circular cylindrical resonators. Similarly to the method of Armaroli *et al.* [24], we use 1D modes that depend on z and analytic solutions in r and θ. Instead of Fourier series, we use the Chebyshev pseudospectral method [27] to discretize z, calculate the 1D modes, and set up the nonlinear matrix eigenvalue problem. Our choice is motivated by the advantage of the Chebyshev pseudospectral method shown in numerical studies of diffraction gratings [28,29]. Our method is applicable to multilayered cylinders embedded in a multilayered surrounding medium. It also gives rise to nonlinear matrix eigenvalue problems, but the matrix size is small. In addition, we develop a robust procedure to reduce the nonlinear matrix eigenvalue problem to a scalar equation, so the complex frequencies of the resonant modes are simply solutions of the scalar equation. For metallic cylinders, analytic models for the dielectric functions of metals are needed. For gold, we show that the critical point (CP) model [30,31] gives satisfactory results. Numerical examples are presented to validate and illustrate our method.

II. VERTICAL MODE EXPANSIONS

We consider a circular cylinder of radius a and height h with its bottom in the xy plane (at $z = 0$) and its axis aligned with the z axis. The dielectric function in the cylindrical region given by $r < a$ (r is the horizontal radial variable) is allowed to be a general function of z and ω, i.e., $\varepsilon = \varepsilon^{(0)}(z, \omega)$, where ω is the angular frequency. The medium outside the cylindrical region can also be layered and its dielectric function is given by $\varepsilon = \varepsilon^{(1)}(z, \omega)$ for $r > a$. In addition, we assume both $\varepsilon^{(0)}$ and $\varepsilon^{(1)}$ become the same constants for $z > h$ and for $z < 0$, respectively.

For scattering problems with a given incident wave at a given real frequency ω, the vertical mode expansion method (VMEM) is very natural and easy to implement [32]. After expanding the incident wave to components that depend on the horizontal angle θ as $e^{im\theta}$ for integers m, the original 3D problem is reduced to independent 2D problems in r and z. For each m, the wave field inside and outside the cylindrical region can be further expanded in corresponding vertical modes which are functions of z. The expansion coefficients satisfy a linear system with a $(4N) \times (4N)$ coefficient matrix, where N is the number of points for discretizing z. Different approaches can be used to solve the vertical modes and to set up the linear systems. The VMEM of Ref. [32] is based on the Chebyshev pseudospectral method [27].

We use VMEM to formulate a nonlinear eigenvalue problem for resonant modes. With a discretization in z, the 1D structure given by $\varepsilon^{(l)}$ (for $l = 0$ or 1) has $2N$ numerically calculated vertical modes $\phi_j^{(l,p)}(z)$ with propagation constants $\eta_j^{(l,p)}$ for $j \in \{1, 2, \ldots, N\}$ and $p \in \{e, h\}$. The cases $p = e$ and $p = h$ correspond to the E and H polarizations, respectively. These vertical modes depend on ω. If a resonant mode depends on θ as $e^{im\theta}$, then its vertical components can be approximated by

$$H_z = e^{im\theta} \sum_{j=1}^{N} c_{j,m}^{(0,e)} \phi_j^{(0,e)}(z) \frac{J_m\left(\eta_j^{(0,e)} r\right)}{J_m\left(\eta_j^{(0,e)} a\right)}, \quad r < a,$$

$$E_z = \frac{e^{im\theta}}{\varepsilon^{(0)}(z)} \sum_{j=1}^{N} c_{j,m}^{(0,h)} \phi_j^{(0,h)}(z) \frac{J_m\left(\eta_j^{(0,h)} r\right)}{J_m\left(\eta_j^{(0,h)} a\right)}, \quad r < a,$$

$$H_z = e^{im\theta} \sum_{j=1}^{N} c_{j,m}^{(1,e)} \phi_j^{(1,e)}(z) \frac{H_m^{(1)}\left(\eta_j^{(1,e)} r\right)}{H_m^{(1)}\left(\eta_j^{(1,e)} a\right)}, \quad r > a,$$

$$E_z = \frac{e^{im\theta}}{\varepsilon^{(1)}(z)} \sum_{j=1}^{N} c_{j,m}^{(1,h)} \phi_j^{(1,h)}(z) \frac{H_m^{(1)}\left(\eta_j^{(1,h)} r\right)}{H_m^{(1)}\left(\eta_j^{(1,h)} a\right)}, \quad r > a,$$

where J_m is the Bessel function of first kind and order m and $H_m^{(1)}$ is the Hankel function of first kind and order m. The horizontal components H_τ and E_τ (tangential to the boundary of the cylinder at $r = a$) can also be written down, and they involve the derivatives of $\phi_j^{(l,p)}(z)$ [32]. The continuity of H_z, E_z, H_τ, and E_τ at $r = a$ and the N discretization points of z gives rise to a homogeneous linear system

$$\mathbf{A}_m(\omega)\, \mathbf{c}_m = \mathbf{0}, \tag{1}$$

where $\mathbf{c}_m$ is a column vector of length $4N$ for $c_{j,m}^{(l,p)}$, $j \in \{1, 2, \ldots, N\}$, $l \in \{0, 1\}$, and $p \in \{e, h\}$. Since all $\phi_j^{(l,p)}$ and $\eta_j^{(l,p)}$ depend on ω, the matrix $\mathbf{A}_m$ also depends on ω. Equation (1) is a fully nonlinear matrix eigenvalue problem. A resonant mode corresponds to a complex ω such that $\mathbf{A}_m$ is singular. The wave field of the mode can be constructed from a nonzero vector $\mathbf{c}_m$ satisfying Eq. (1).

Notice that the right-hand side of Eq. (1) is zero, since resonant modes are nonzero solutions without incident waves and sources. For scattering problems with a given incident field at a given frequency, the VMEM [32] gives rise to

$$\mathbf{A}_m(\omega)\, \mathbf{c}_m = \mathbf{b}_m, \tag{2}$$

where $\mathbf{b}_m$ is a vector with four blocks related to the z and τ components of electromagnetic fields of some reference solutions (induced by the incident wave), and each block is a vector of length N corresponding to the N discretization points of z.

Nonlinear eigenvalue problems can be solved by local iterative methods or global contour integration methods [33,34]. A local iterative method relies on a scalar function $f(\omega)$, such that $f(\omega) = 0$ if and only if $\mathbf{A}_m(\omega)$ is singular. Choices of f include the determinant of $\mathbf{A}_m$, the smallest singular value of $\mathbf{A}_m$, the smallest eigenvalue (in magnitude) of $\mathbf{A}_m$, etc. The determinant is usually not a good indicator for singularities of a matrix, unless the size of the matrix is very small. The smallest singular value or eigenvalue are better indicators, but they can still be difficult to use if the matrix $\mathbf{A}_m$ is ill conditioned (close to singular) even when ω is away from a complex resonant frequency. Cheng *et al.* [35] suggested to use

$$f(\omega) = \frac{1}{\mathbf{a}^T \mathbf{A}_m^{-1} \mathbf{b}}, \tag{3}$$

where **a** and **b** are given vectors independent of ω. If **a** and **b** are chosen randomly, as suggested by the authors of Ref. [35], then the function f above can be rather oscillatory, and an iterative method may have difficulty to converge, even when a good initial guess is available.

The contour integration methods are more robust. They can be used to calculate all resonant modes inside a domain in the complex ω plane, without the need for any initial guesses. Equation (3) suggests that a solution ω of $f(\omega) = 0$ is a pole of a complex function $g(\omega) = \mathbf{a}^T \mathbf{A}_m^{-1} \mathbf{b}$, assuming $\mathbf{A}_m$ is analytic in ω and g is analytic in ω except at the poles corresponding to the complex resonant frequencies. Therefore, contour integrals can be used to determine the poles of g based on the residue theorem. The contour integration methods of Refs. [33,34] are more robust since they replace the vectors **a** and **b** by matrices, but they are not very efficient, since they need to evaluate the integral on the chosen contours to high accuracy and these contours cannot be too close to the complex resonant frequencies.

We use a local iterative method based on the $f(\omega)$ given in Eq. (3), but choose **a** and **b** as simple column vectors with only one or two nonzero entries. The vectors **a** and **b** are chosen such that $f(\omega)$ is smooth near the complex resonant frequency. Consider E_z and H_z along the vertical boundary of the cylinder at $r = a$. If H_z is expected to be strong at $z = z_l$ (one of the discretization points of z), then we can put a nonzero entry 1 in the vector **b** at the position corresponding to H_z at z_l. If H_z is expected to have a significant overlap with the first E-polarized vertical mode, then we place a nonzero entry 1 in the vector **a** to pick up the coefficient of $\phi_1^{(0,e)}$. In that case, $\mathbf{a}^T \mathbf{A}_m^{-1} \mathbf{b} = c_{1,m}^{(0,e)}$ and $f(\omega) = 1/c_{1,m}^{(0,e)}$. If H_z has a more significant overlap with the second vertical mode, then we choose **a** such that $f(\omega) = 1/c_{2,m}^{(0,e)}$. Similarly, if E_z is the dominant z component, then a nonzero entry of **b** is put in the block corresponding to E_z, and **a** is chosen such that $f(\omega) = 1/c_{j,m}^{(0,h)}$ where j is usually 1 or 2, depending on which vertical mode has a more significant overlap with E_z. If the structure has a reflection symmetry in z, then the resonant mode is either symmetric or antisymmetric in z, and we can use a vector **b** with two (symmetrically positioned) nonzero entries, either 1 and 1 or 1 and -1, to excite symmetric or antisymmetric modes, respectively. The equation $f(\omega) = 0$ can be solved by standard iterative methods such as the secant method. With this strategy for choosing **a** and **b**, the method exhibits excellent global convergence, and resonant modes can be found even when the initial guesses are not very accurate.

For resonators with a dispersive material, it is necessary to use an analytic model for its dielectric function, since a resonant mode has a complex frequency, but measured data for the dielectric function are only available for real frequencies. Analytic models for dielectric functions of metals and other dispersive materials are widely used in time-domain numerical simulations. The simplest one is the Drude model, but it is only accurate in a limited frequency range. The multipole Lorentz-Drude models are more appropriate [16,17]. For gold, the CP model is only slightly more complicated than the Drude model, and it gives a good fit for a wide range of frequencies [30,31]. Some details on the CP model are given in the Appendix. Notice that all analytic models are obtained by fitting measured data for real frequencies, it is not clear how accurate these models are for complex frequencies. It is possible that fitting real-frequency data with too many terms can only give less accurate approximations for complex frequencies. We believe the CP model is highly appropriate for computing resonant modes of gold resonators in the optical frequency range.

TABLE I. Resonant wavelength Re(λ) (in μm) and quality factor Q for selected modes of a microdisk resonator.

	Armaroli [24]		Li [26]		This work	
Mode	Re(λ)	Q	Re(λ)	Q	Re(λ)	Q
$TE_{1,5}$	1.5735	16	1.5728	19	1.5729	20
$TE_{1,6}$	1.4019	34	1.4016	41	1.4016	41
$TE_{1,7}$	1.2655	82	1.2665	89	1.2665	90
$TE_{1,8}$	1.1583	175	1.1574	199	1.1574	200
$TE_{1,9}$	1.0694	350	1.0673	457	1.0674	456
$TE_{1,10}$	0.9938	828	0.9914	1059	0.9915	1061
$TM_{1,6}$	1.3079	25	1.3052	25	1.3053	25
$TM_{1,7}$	1.2045	52	1.1998	51	1.1998	51
$TM_{1,8}$	1.1122	105	1.1112	107	1.1112	107
$TM_{1,9}$	1.0358	215	1.0356	237	1.0357	238
$TM_{1,10}$	0.9706	536	0.9703	549	0.9704	548
$TM_{1,11}$	0.9132	1254	0.9130	1303	0.9131	1303

III. DIELECTRIC RESONATORS

To validate and illustrate our method, we present a few numerical examples for cylindrical dielectric resonators in this section. The first example is a microdisk with a dielectric constant $\varepsilon = 10.24$ surrounded by a dielectric medium with $\varepsilon = 2.25$. The radius and height of the microdisk are $a = 0.77$ μm and $h = 0.24$ μm, respectively. This example was previously analyzed by Armaroli *et al.* [24] and Li *et al.* [26] using special FMMs with 1D vertical and radial modes, respectively. PMLs are used in these works to periodize the z or r directions. In our method, the z variable is truncated to an interval of 1.92 μm with a total of five layers. The top and bottom layers are PMLs with a thickness of 0.6 μm. The middle layer corresponds to the microdisk of height h. Between the PMLs and the middle layer are dielectric layers of 0.24 μm. Since the bottom of the microdisk is in the $z = 0$ plane, the PML above the microdisk is a layer from $z_{\text{pml}} = 0.48$ μm to $z_{\text{end}} = 1.08$ μm, where z is replaced by

$$\hat{z} = z + S \int_{z_{\text{pml}}}^{z} \left(\frac{\tau - z_{\text{pml}}}{z_{\text{end}} - z_{\text{pml}}} \right)^2 d\tau. \tag{4}$$

The PML below the microdisk is similarly defined. The z variable is discretized by Chebyshev points in five subintervals with a total of $N = 108$ discretization points, and the parameter S for the PMLs is $S = 3 + 7i$. Our results are listed in Table I for comparison with those of Refs. [24,26]. For all three methods, we list the resonant wavelength Re(λ), where $\lambda = 2\pi c/\omega$ is the complex wavelength and c is the speed of light in vacuum and the quality factor

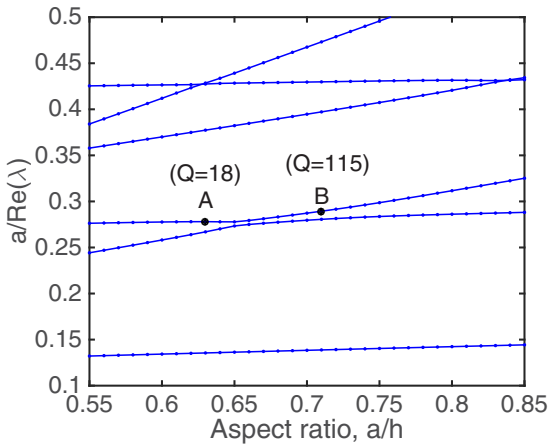

FIG. 1. Normalized resonant frequencies of a few resonant modes on an AlGaAs cylinder of varying aspect ratio.

$Q = -0.5\mathrm{Re}(\omega)/\mathrm{Im}(\omega) = 0.5\mathrm{Re}(\lambda)/\mathrm{Im}(\lambda)$. The quasi-transverse-electric (quasi-TE) and quasi-transverse-magnetic (quasi-TM) modes have dominant H_z and E_z components respectively, and are denoted as $\mathrm{TE}_{j,m}$ and $\mathrm{TM}_{j,m}$, where m is the azimuthal index and j is the mode index. The case $j = 1$ corresponds to a vertical profile with a single field maximum located at the middle of the microdisk. Large values of m correspond to whispering-gallery modes with high Q factors. Our results agree very well with those of Li *et al.* [26]. Notice that the resonant wavelength decreases as m increases, and only the first mode in the table, i.e., $\mathrm{TE}_{1,5}$, has a resonant wavelength larger than the diameter $2a = 1.54\ \mu$m.

Recently, subwavelength dielectric structures supporting high-Q resonances have been designed by relating them to periodic structures with bound states in the continuum [7]. In particular, resonant modes with quality factors over 100 have been found on subwavelength circular cylinders of AlGaAs and they have been used to enhance nonlinear optical effects [8]. Using our method presented in the previous section, we calculate a few resonant modes for a circular AlGaAs cylinder surrounded by air, assuming the dielectric constant of AlGaAs is $\varepsilon = 10.73$. In Fig. 1, we show the first six symmetric quasi-TE modes of azimuthal order $m = 0$ for different aspect ratio a/h. The vertical axis of Fig. 1 is the real normalized resonant frequency $\mathrm{Re}(\omega)a/(2\pi c) = a/\mathrm{Re}(\lambda)$. Our results agree very well with those of Carletti *et al.* [8]. In our calculations, the vertical variable z is truncated by PMLs and discretized by $N = 108$ points. In Fig. 1, two points are highlighted on the curve corresponding to the third smallest resonant frequency. The points A and B correspond to resonant modes with quality factors $Q = 18$ and $Q = 115$, respectively. The field profiles for these two points are shown in Fig. 2, where **H** is the magnetic field multiplied by the free space impedance, so that **H** and electric field **E** have the same physical units. For both A and B, the resonant wavelength is significantly larger than the diameter and height of the cylinder.

If the dielectric constant of the cylinder is further increased, then the quality factors of the resonant modes can be even larger. For example, if the dielectric constant of the cylinder is changed to $\epsilon = 11.56$ (for silicon) and the surrounding medium is still air ($\epsilon = 1$), then there is a high-Q resonant

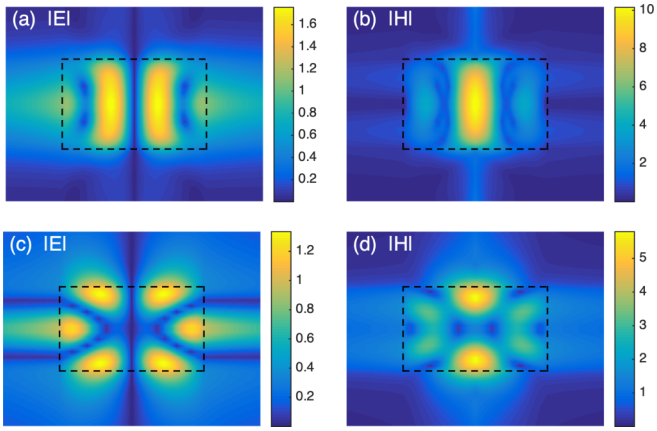

FIG. 2. Magnitudes of the electric field **E** and scaled magnetic field **H** on the xz plane for the AlGaAs cylinder at points A and B in Fig. 1, where (a) and (b) are for point A and (c) and (d) are for point B.

mode for aspect ratio $a/h = 0.88211$ and the quality factor is $Q \approx 179.427$. The normalized complex frequency of this resonant mode is $\omega a/(2\pi c) = a/\lambda = 0.4256205–0.001186053\mathrm{i}$. Its electromagnetic field patterns are shown in Fig. 3. Notice that the diameter and height of the cylinder are still smaller than the resonant wavelength.

IV. METALLIC RESONATORS

In this section, we calculate some resonant modes for circular metallic cylinders of different sizes. The first example is a gold nanorod of radius $a = 15$ nm and height $h = 100$ nm, embedded in a dielectric medium of $\varepsilon = 2.25$. This example was previously analyzed using a finite element method [36] and a FMM [23,25]. In these works, a particular resonant mode with azimuthal order $m = 0$ was carefully studied, while the dielectric function of gold is approximated by a Drude model,

$$\varepsilon(\omega) = \varepsilon_\infty - \frac{\omega_p^2}{\omega^2 + i\Gamma\omega},$$

with parameters $\varepsilon_\infty = 1$, $\omega_p = 1.26 \times 10^{16}$ rad/s, and $\Gamma = 1.41 \times 10^{14}$ rad/s. These parameters are chosen to fit the measured data of Ref. [37]. The complex wavelength of that mode is approximately $0.9177210 + i0.0469092\ \mu$m [36] or $0.9173666 + i0.0468896\ \mu$m [25]. Using the same Drude model, we calculate the resonant mode with our method and obtain the complex wavelength $\lambda = 0.9176863 +$

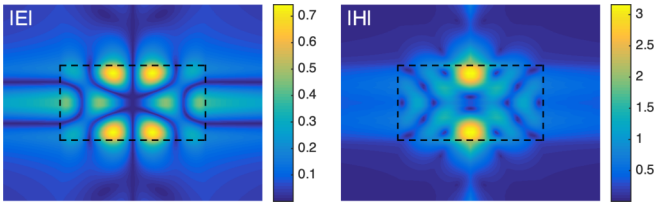

FIG. 3. Magnitudes of the electric field **E** (left) and scaled magnetic field **H** (right) on the xz plane of a resonant mode for a silicon cylinder with aspect ratio $a/h = 0.88211$.

$i0.0469084$ μm. Our result has an excellent agreement with the FEM result [36] and a good agreement with FMM result [25]. Due to field singularity along the sharp edges and the large field gradient at the surface of the nanorod, numerical methods typically exhibit a slow convergence, and it is difficult to assess the accuracy of these solutions. To obtain our result, we used $N = 265$ points to discretize the z variable truncated to the interval $(-1, 1.1)$ μm, where the bottom of the nanorod is at $z = 0$.

Next, we calculate the resonant modes of a gold cylinder with radius $a = 40$ nm and height $h = 50$ nm, assuming it is surrounded by a homogeneous medium with dielectric constant $\varepsilon = 2.25$. In order to find resonant modes with different resonant frequencies, it is desirable to use an analytic model (for the dielectric function of gold) which is accurate for a wider frequency range. One possibility is to use the Lorentz-Drude model [16,17]. We choose to use the relatively simple CP model [30,31]. Some details of the CP model are given in the Appendix. It should be pointed out that all these models are obtained by fitting measured data for real frequencies, but what is needed is a formula for the dielectric function on the complex ω plane (at least near the real axis). This is a difficult task, since the measured data on the real ω axis have only limited accuracy, and, more importantly, there is no guarantee that a formula fitting real ω data very well remains accurate for complex ω. From that perspective, a simple formula, such as the CP model, that fits the real ω data reasonably well over a sufficient large frequency range is probably the right choice. Based on the CP model, we obtain a symmetric resonant mode of azimuthal order $m = 1$ with complex wavelength $\lambda = 0.6369 + i0.04402$ μm and quality factor $Q = 7.2342$. For this calculation, the vertical variable z is truncated to $(-0.3, 0.35)$ μm by PMLs, and the boundaries among the bottom and top PMLs, dielectric layers, and the cylinder are located at $z = -0.1$, 0, 0.05, and 0.15 μm. The PML above the cylinder is a layer from $z_{\text{pml}} = 0.15$ μm to $z_{\text{end}} = 0.35$ μm, and the complex variable $\hat{z}$ is defined in Eq. (4) for $S = 7 + 5i$. The bottom PML is similar. The five subintervals of z are discretized by 47, 25, 13, 25, and 47 points, respectively. The total number of discretization points for z is $N = 157$.

In order to provide some justification for our choice of the CP model, we calculate the scattering spectrum of the gold cylinder for normal incident plane waves. In Fig. 4, we show the normalized scattering cross section as a function of the incident wavelength. The results are obtained using the VMEM for scattering problems as formulated in Ref. [32]. The red solid line and the blue circles are results obtained using the CP model and the measured data of Johnson and Christ [38]. Due to the circular geometry of the cylinder, a normal incident plane wave (with a wave vector parallel to the z axis) produces a scattering field with an azimuthal dependence of $\sin(\theta)$ and $\cos(\theta)$. Therefore, the normal incident plane wave can only excite resonant modes with azimuthal order $m = \pm 1$. The peak of the scattering spectrum is located at 0.641 μm, and it is close to the resonant wavelength $\text{Re}(\lambda) = 0.6369$ μm calculated earlier. By measuring the difference in wavelengths at which the normalized scattering cross section reaches its half-maximum, an approximation of the quality factor can be obtained, and it is about 7.54. The agreement with the directly calculated value $Q = 7.2342$ is acceptable. Since the quality factor is quite small, it is impossible to accurately extract the resonant wavelength and quality factor from the scattering spectrum. Based on these calculations, we believe that the CP model can give satisfactory results for resonant modes of gold resonators in the optical frequency range.

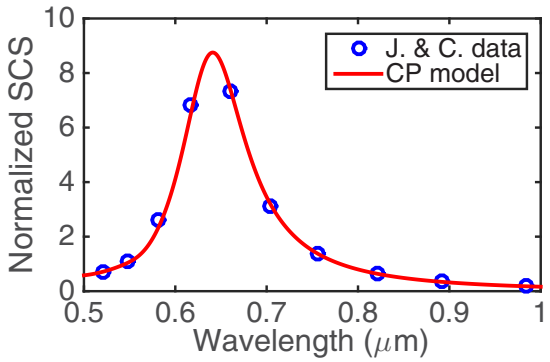

FIG. 4. Normalized scattering cross section of a gold circular cylinder with radius 40 nm and height 50 nm for a normal incident plane wave.

V. CONCLUSION

Open circular cylindrical resonators appear in numerous nanophotonics applications. A special numerical method is developed for computing resonant modes of (possibly multilayered) circular cylinders of finite height embedded in a possibly layered background. The method relies on expansions of the field in 1D modes which are functions of z, establishes 1D eigenvalue problems using Chebyshev pseudospectral method, and includes a new procedure for solving the resulting nonlinear eigenvalue problems. The method is further applied to determine the aspect ratio of subwavelength silicon cylinder with a high-Q resonance ($Q \approx 179.427$). It is also used to analyze a gold nanocylinder. It is shown that the resonant wavelength and Q factor calculated directly using the CP model (for the dielectric function of gold) agree reasonably well with those extracted from the scattering spectrum.

Although general numerical methods, such as the FEM, are available for computing resonant modes even when the media are dispersive, our method is simple, efficient, and robust. For scattering problems, the VMEM is applicable to more general structures including cylinders with arbitrary cross sections [39], multiple cylinders [40,41], and periodic arrays of cylinders [42]. We are extending the method for computing resonant modes for such more general structures.

ACKNOWLEDGMENTS

The first author acknowledges support from the National Natural Science Foundation of China (Grant No. 11847156). The second author acknowledges support from the Research Grants Council of Hong Kong Special Administrative Region, China (Grant No. CityU 11304117).

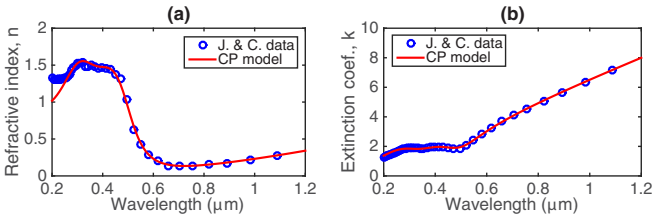

FIG. 5. Comparison of the CP model and measured data of Ref. [38] for gold. Panels (a) and (b) show real and imaginary parts of $\sqrt{\varepsilon} = n + ik$.

APPENDIX

The CP model [30,31] for gold is

$$\varepsilon(\omega) = \varepsilon_\infty - \frac{\omega_p^2}{\omega^2 + i\Gamma\omega} + \sum_{j=1}^{2} G_j(\omega),$$

where the first two terms in the right-hand side above is the Drude model, and

$$G_j(\omega) = C_j\left(\frac{e^{i\phi_j}}{\omega_j - \omega - i\Gamma_j} + \frac{e^{-i\phi_j}}{\omega_j + \omega + i\Gamma_j}\right).$$

In the above, ε_∞, ω_p, Γ, ω_j, Γ_j, ϕ_j, and C_j are parameters chosen to fit the measured data of Ref. [38], and they are

$$\begin{aligned}
&\varepsilon_\infty = 1.54, && \phi_1 = \phi_2 = -\pi/4,\\
&\omega_p = 1.31815 \times 10^{16}, && \Gamma = 1.29997 \times 10^{14}\\
&C_1 = 5.09339 \times 10^{15}, && C_2 = 6.37985 \times 10^{15}\\
&\omega_1 = 4.01054 \times 10^{15}, && \omega_2 = 5.79986 \times 10^{15},\\
&\Gamma_1 = 9.92082 \times 10^{14}, && \Gamma_2 = 1.77826 \times 10^{15}.
\end{aligned}$$

The unit for ω_p, Γ, C_j, ω_j, and Γ_j is rad/s. In Fig. 5, we compare the CP model for gold with the data of Ref. [38] for the real and imaginary parts of $\sqrt{\varepsilon} = n + ik$.

[1] P. Lalanne, W. Yan, K. Vynck, C. Sauvan, and J.-P. Hugonin, Light interaction with photonic and plasmonic resonances, Laser Photon. Rev. **12**, 1700113 (2018).

[2] M. Soltani, S. Yegnanarayanan, and A. Adibi, Ultra-high Q planar silicon microdisk resonators for chip-scale silicon photonics, Opt. Expr. **15**, 4694 (2007).

[3] P. Genevet, F. Capasso, F. Aieta, M. Khorasaninejad, and R. Devlin, Recent advances in planar optics: From plasmonic to dielectric metasurfaces, Optica **4**, 139 (2017).

[4] M. Khorasaninejad and F. Capasso, Metalenses: Versatile multifunctional photonic components, Science **358**, eaam8100 (2017).

[5] V.-C. Su, C. H. Chu, G. Sun, and D. P. Tsai, Advances in optical metasurfaces: Fabrication and applications, Opt. Expr. **26**, 13148 (2018).

[6] S. Shrestha, A. C. Overvig, M. Lu, A. Stein, and N. Yu, Broadband achromatic dielectric metalenses, Light: Sci. Appl. **7**, 85 (2018).

[7] M. V. Rybin, K. L. Koshelev, Z. F. Sadrieva, K. B. Samusev, A. A. Bogdanov, M. F. Limonov, and Y. S. Kivshar, High-Q Supercavity Modes in Subwavelength Dielectric Resonators, Phys. Rev. Lett. **119**, 243901 (2017).

[8] L. Carletti, K. Koshelev, C. De Angelis, and Y. Kivshar, Giant Nonlinear Response at the Nanoscale Driven by Bound States in the Continuum, Phys. Rev. Lett. **121**, 033903 (2018).

[9] M. Tsuji, H. Shigesawa, and K. Takiyama, On the complex resonant frequency of open dielectric resonators, IEEE Trans. Microwave Theory Techn. **31**, 392 (1983).

[10] A. W. Glisson, D. Kajfez, and J. James, Evaluation of modes in dielectric resonators using a surface integral equation formulation, IEEE Trans. Microwave Theory Techn. **31**, 1023 (1983).

[11] S. Hyun, J. Hwang, Y. Lee, and S. Kim, Computation of resonant modes of open resonators using the FEM and the anisotropic perfectly matched layer boundary condition, Microwave Opt. Technol. Lett. **16**, 352 (1997).

[12] J.-K. Hwang, S.-B. Hyun, H.-Y. Ryu, and Y.-H. Lee, Resonant modes of two-dimensional photonic bandgap cavities determined by the finite-element method and by use of the anisotropic perfectly matched layer boundary condition, J. Opt. Soc. Am. B **15**, 2316 (1998).

[13] S. Kim and J. E. Pasciak, The computation of resonances in open systems using a perfectly matched layer, Math. Comput. **78**, 1375 (2009).

[14] G. Bao Z. Chen, and H. Wu, Adaptive finite-element method for diffraction gratings, J. Opt. Soc. Am. A **22**, 1106 (2005).

[15] J. P. Berenger, A perfectly matched layer for the absorption of electromagnetic waves, J. Comput. Phys. **114**, 185 (1994).

[16] A. Raman and S. Fan, Photonic Band Structure of Dispersive Metamaterials Formulated as a Hermitian Eigenvalue Problem, Phys. Rev. Lett. **104**, 087401 (2010).

[17] W. Yan, R. Feggiani, and P. Lalanne, Rigorous modal analysis of plasmonic nanoresonators, Phys. Rev. B **97**, 205422 (2018).

[18] D. A. Powell, Resonant dynamics of arbitrarily shaped meta-atoms, Phys. Rev. B **90**, 075108 (2014).

[19] L. Li, New formulation of the Fourier modal method for crossed surface-relief gratings, J. Opt. Soc. Am. A **14**, 2758 (1997).

[20] E. Silberstein, P. Lalanne, J.-P. Hugonin, and Q. Cao, Use of grating theories in integrated optics, J. Opt. Soc. Am. A **18**, 2865 (2001).

[21] G. Granet and J.-P. Plumey, Parametric formulation of the Fourier modal method for crossed surface-relief gratings, J. Opt. A **4**, S145 (2002).

[22] P. Lalanne, J. P. Hugonin, and J. S. Gerard, Electromagnetic study of the quality factor of pillar microcavities in the small diameter limit, Appl. Phys. Lett. **84**, 4726 (2004).

[23] C. Sauvan, J. P. Hugonin, I. S. Maksymov, and P. Lalanne, Theory of the Spontaneous Optical Emission of Nanosize Photonic and Plasmon Resonators, Phys. Rev. Lett. **110**, 237401 (2013).

[24] A. Armaroli, A. Morand, P. Benech, G. Bellanca, and S. Trillo, Three-dimensional analysis of cylindrical microresonators based on the aperiodic Fourier modal method, J. Opt. Soc. Am. A **25**, 667 (2008).

[25] F. Bigourdan, J.-P. Hugonin, and P. Lalanne, Aperiodic-Fourier modal method for analysis of body-of-revolution photonic structures, J. Opt. Soc. Am. A **31**, 1303 (2014).

[26] Y. Li, H. Liu, H. Jia, F. Bo, G. Zhang, and J. Xu, Fully vectorial modeling of cylindrical microresonators with aperiodic Fourier modal method, J. Opt. Soc. Am. A **31**, 2459 (2014).

[27] L. N. Trefethen, *Spectral Methods in MATLAB* (Society for Industrial and Applied Mathematics, Philadelphia, PA, 2000).

[28] D. Song, L. Yuan, and Y. Y. Lu, Fourier-matching pseudospectral modal method for diffraction gratings, J. Opt. Soc. Am. A **28**, 613 (2011).

[29] G. Granet, Fourier-matching pseudospectral modal method for diffraction gratings: Comment, J. Opt. Soc. Am. A **29**, 1843 (2012).

[30] P. G. Etchegoin, E. C. Le Ru, and M. Meyer, An analytic model for the optical properties of gold, J. Chem. Phys. **125**, 164705 (2006).

[31] P. G. Etchegoin, E. C. Le Ru, and M. Meyer, Erratum: An analytic model for the optical properties of gold, J. Chem. Phys. **127**, 189901 (2007).

[32] X. Lu and Y. Y. Lu, Analyzing bull's eye structures by a vertical mode expansion method with rotational symmetry, J. Opt. Soc. Am. B **32**, 2294 (2015).

[33] J. Asakura, T. Sakurai, H. Tadano, T. Ikegami, and K. Kimura, A numerical method for nonlinear eigenvalue problems using contour integrals, JSIAM Lett. **1**, 52 (2009).

[34] W.-J. Beyn, An integral method for solving nonlinear eigenvalue problems, Linear Algeb. Appl. **436**, 3839 (2012).

[35] H. Cheng, W. Y. Crutchfield, M. Doery, and L. Greengard, Fast, accurate integral equation methods for the analysis of photonic crystal fibers I: Theory, Opt. Expr. **12**, 3791 (2004).

[36] Q. Bai, M. Perrin, C. Sauvan, J.-P. Hugonin, and P. Lalanne, Efficient and intuitive method for the analysis of light scattering by a resonant nanostructure, Opt. Expr. **21**, 27371 (2013).

[37] E. D. Palik, *Handbook of Optical Constants of Solids* (Academic Press, New York, 1985).

[38] P. B. Johnson and R. W. Christy, Optical constants of the noble metals, Phys. Rev. B **6**, 4370 (1972).

[39] H. Shi and Y. Y. Lu, Efficient vertical mode expansion method for scattering by arbitrary layered cylindrical structures, Opt. Expr. **23**, 14618 (2015).

[40] X. Lu and Y. Y. Lu, Efficient method for analyzing multiple circular cylindrical nanoparticles on a substrate, J. Opt. **18**, 055604 (2016).

[41] H. Shi, Y. Y. Lu, and Q. Du, Analyzing bowtie structures with sharp tips by a vertical mode expansion method, Opt. Expr. **26**, 32346 (2018).

[42] H. Shi, X. Lu, and Y. Y. Lu, Vertical mode expansion method for numerical modeling of biperiodic structures, J. Opt. Soc. Am. A **33**, 836 (2016).